

# J-CAPA : JOINT CHANNEL AND PYRAMID ATTENTION IMPROVES MEDICAL IMAGE SEGMENTATION

*Marzia Binta Nizam*

*Marian Zlateva*

*James Davis*

Department of Computer Science, University of California, Santa Cruz, CA

## ABSTRACT

Medical image segmentation is crucial for diagnosis and treatment planning. Traditional CNN-based models, like U-Net, have shown promising results but struggle to capture long-range dependencies and global context. To address these limitations, we propose a transformer based architecture that jointly applies Channel Attention and Pyramid Attention mechanisms to improve multi-scale feature extraction and enhance segmentation performance for medical images. Increasing model complexity requires more training data, and we further improve model generalization with CutMix data augmentation. Our approach is evaluated on the Synapse multi-organ segmentation dataset, achieving a 6.9% improvement in Mean Dice score and a 39.9% improvement in Hausdorff Distance (HD95) over an implementation without our enhancements. Our proposed model demonstrates improved segmentation accuracy for complex anatomical structures, outperforming existing state of the art methods.

**Index Terms**— Medical Image Segmentation, TransU-Net, Transformer

## 1. INTRODUCTION

Medical image segmentation is a fundamental task in clinical applications, providing the precise identification of anatomical structures critical for various diagnoses and treatments. However, it remains challenging due to the varying size, shape, and appearance of different organs and pathologies. While convolutional neural networks (CNNs), like U-Net[1] and its variants[2, 3, 4], have shown strong results, they often struggle to model long-range dependencies and global context effectively—key factors for segmenting complex structures.

To address these limitations, Transformer-based architectures have been explored in computer vision. Transformers use self-attention mechanisms to capture global context and long-range dependencies, which offers advantages over traditional CNNs. The Vision Transformer (ViT) and its adaptations have demonstrated significant improvements in medical image segmentation.

We propose a method called J-CaPA that integrates joint attention mechanisms—Channel Attention and Pyramid Attention—into a Transformer-based U-Net model. These

mechanisms improve feature representation by effectively capturing both local and global contexts. These attention layers increase the number of weights, so we increase data augmentation using CutMix to insure the model does not overfit.

Our approach is evaluated on the Synapse<sup>1</sup> multi-organ segmentation dataset, which consists of 30 abdominal CT scans with annotations for several organs, including the aorta, gallbladder, kidneys, liver, pancreas, spleen, and stomach. Our model achieved a 6.9% improvement in Mean Dice score and a 39.9% reduction in Hausdorff Distance (HD95) over an implementation without our enhancements. Notably, the segmentation of organs such as the gallbladder, kidneys, and pancreas showed marked improvement, indicating the model’s ability to handle complex anatomical structures effectively.

Evaluation results indicate that our architecture performs better than multiple state of the art comparison methods. Importantly, ablation studies show that neither Channel Attention nor Pyramid Attention used independently results in optimal performance. The key contribution of this paper is showing that jointly applying these attention models is what leads to enhanced medical image segmentation accuracy.

## 2. RELATED WORK

### 2.1. CNN-Based Methods for Medical Image Segmentation

CNNs, including FCNs [5] and U-Net variants [1], have shown strong segmentation performance. U-Net++ [6] narrows the semantic gap using dense skip connections, while Attention U-Net [7] employs attention gates for feature selection. Models like Res-UNet [3] and R2U-Net [4] introduced residual connections to refine segmentation tasks, while DoubleU-Net [8] and specialized networks like PraNet [9] and KiU-Net [2] targeted specific medical challenges. Despite these advances, CNNs still struggle with modeling long-range dependencies. Attempts to integrate self-attention mechanisms [10, 11] improved feature selection but were insufficient in capturing global context. This limitation has shifted interest towards Transformer-based architectures, which excel in combining global and local features.

<sup>1</sup><https://www.synapse.org/Synapse:syn3193805/wiki/89480>

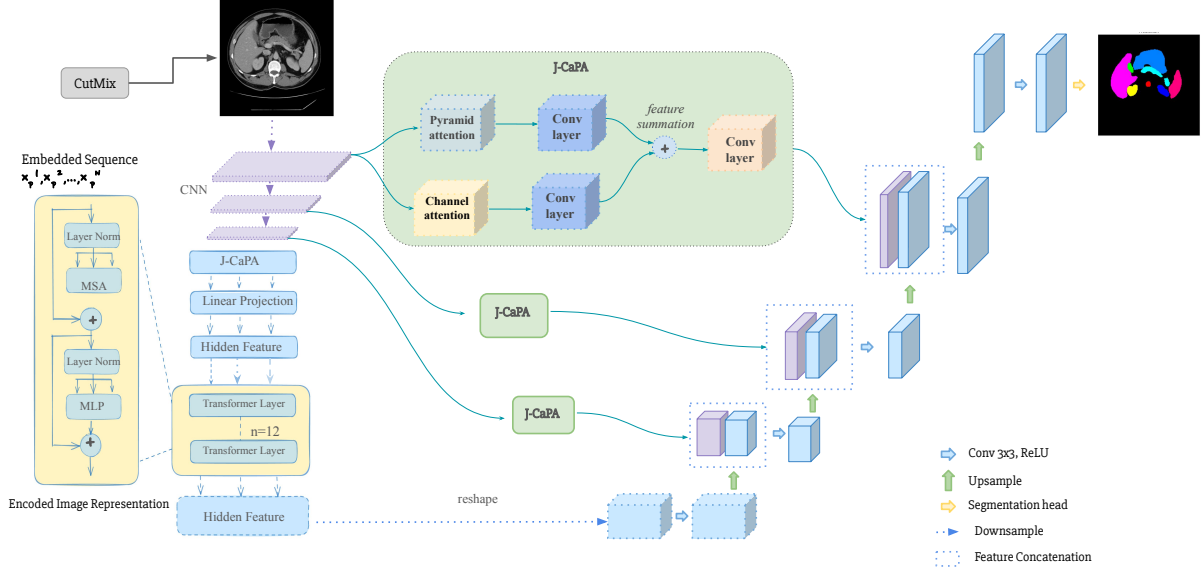


**Fig. 1:** Overview of the proposed framework. Input medical images are processed by a CNN-based encoder, followed by Transformer layers and our Joint Attention blocks (combining Pyramid and Channel Attention). Features at multiple scales are refined by Joint Attention and passed through skip connections to the decoder. The decoder performs CNN-based up-sampling to generate high-resolution segmentation maps, capturing detailed anatomical structures.

## 2.2. Transformer-Based Approaches for Medical Image Segmentation

Transformers, originally developed for natural language processing [12], have recently gained traction in computer vision tasks due to their ability to model long-range dependencies. Vision Transformer (ViT) [13] demonstrated state-of-the-art performance, leading to adaptations for medical image segmentation, such as TransUNet [14], which combines the strengths of both Transformers and CNNs. Further improvements were made with models like Swin-Unet [15] and DS-TransUNet [16], which introduced hierarchical Transformer blocks and enhanced feature fusion. Other notable models, such as AA-TransUNet [17] and DA-TransUNet [18], explored spatial and channel attention mechanisms.

Transformer base large models, including Segment Anything Model (SAM) [19], SegGPT [20], and STU-Net [21], have gained attention for their zero-shot generalization capabilities. However, their performance in medical image segmentation has been limited due to a lack of domain-specific training data. Adaptations like MedSAM [22] and Medical SAM Adapter [23] have fine-tuned SAM for medical datasets through prompt-based methods, while prompt-free approaches such as AutoSAM [24] have attempted to eliminate the need for prompts. SAMed [25] enhances SAM's segmentation performance by integrating LoRA layers [26] into the model.

Our approach builds on these advancements by integrating Channel and Pyramid Attention into a transformer-based

architecture, enabling multi-scale feature extraction tailored for medical image segmentation.

## 3. METHODOLOGY

### 3.1. Model Architecture Overview

The overall architecture of our model is a Transformer based structure, with an encoder-decoder design as shown in Figure 1. The encoder employs Transformer blocks to capture global context, while the decoder reconstructs detailed segmentation maps. The encoder features a modified ResNetV2 backbone that extracts hierarchical features through convolutional layers and residual bottleneck blocks. These features are refined by joint attention modules to enhance both local and global context. The decoder then uses upsampling operations to reconstruct segmentation maps from the refined features provided by the attention modules.

### 3.2. Joint Attention Mechanisms

To enhance feature representation, we incorporate two types of attention mechanisms, Channel Attention and Pyramid Attention.

#### 3.2.1. Channel Attention Module

The Channel Attention Module (CAM) was originally introduced for segmenting city street scenes [29] and has also been successfully applied in medical image segmentation tasks [30, 18]. For our work, we take an input feature map  $X \in \mathbb{R}^{B \times C \times H \times W}$ , where  $B$  is the batch size,  $C$  is the number

**Table 1:** Segmentation accuracy of different methods on the Synapse multi-organ CT dataset(Average Dice Similarity Coefficient (DSC) score (%) and average Hausdorff Distance (HD) in mm, along with DSC score (%) for each organ). The best results are highlighted in bold.

Model	Mean Dice $\uparrow$	Mean HD95 $\downarrow$	Aorta	Gallbladder	Kidney (L)	Kidney (R)	Liver	Pancreas	Spleen	Stomach
TransUNet [14]	76.90	32.87	86.80	59.60	81.40	74.00	94.50	54.10	87.30	77.80
TransNorm[27]	78.40	30.25	86.23	65.10	82.18	78.63	94.22	55.34	89.50	76.01
SwinUnet [15]	79.13	21.55	85.47	66.53	83.28	79.61	94.29	56.58	90.66	76.60
DA-TransUnet [18]	79.80	23.48	86.54	65.27	81.70	80.45	94.57	61.62	88.53	79.73
IB-TransUNet[28]	81.05	22.63	88.24	66.25	83.89	79.87	94.63	63.56	90.23	81.75
SAMed[25]	81.88	20.64	87.77	<b>69.11</b>	80.45	79.95	<b>94.8</b>	<b>72.17</b>	88.72	82.06
<b>Ours</b>	<b>82.29</b>	<b>19.74</b>	<b>88.28</b>	63.10	<b>86.00</b>	<b>83.10</b>	94.60	69.30	<b>90.70</b>	<b>83.30</b>

of channels, and H and W are the height and width of the feature map, respectively. CAM computes inter-channel dependencies by reshaping this feature map into  $B \times C \times (H \times W)$ . For each channel, query and key representations are derived by projecting the input into a pair of matrices. Following previous work [18], the energy matrix is normalized using a max-value subtraction technique, and softmax is applied to obtain attention weights. These weights are then used to reweight the value representation of the input, which is then reshaped backed to  $B \times C \times H \times W$ . The final output is obtained by blending the attention-modified features with the original input, controlled by learnable parameter  $\gamma_{CA}$ . Initially set to zero,  $\gamma_{CA}$  is updated during training through backpropagation. As the model trains,  $\gamma_{CA}$  is optimized using gradient descent.

### 3.2.2. Pyramid Attention Module

The Pyramid Attention Module captures multi-scale context by applying attention across different spatial scales [31]. The module processes the input feature map  $X \in \mathbb{R}^{B \times C \times H \times W}$ , denoted as  $X_s$ , where  $s$  represents the scale factor (original size:  $s=1$ , half-size:  $s=0.5$ , and quarter-size:  $s=0.25$ ). For each scale  $s$ , we apply three convolutional layers to produce the *query*, *key*, and *value* representations:

$$Q_s = W_Q X_s, \quad K_s = W_K X_s, \quad V_s = W_V X_s$$

where  $W_Q, W_K \in \mathbb{R}^{C \times C/8}$  are learnable weight matrices, and  $W_V \in \mathbb{R}^{C \times C}$  preserves the original dimensions. Attention weights are computed using dot-product attention, followed by softmax normalization, to capture contextual relationships between spatial positions at each scale. The attention-modified features are then upsampled back to the original resolution and combined with the input feature map using a learnable parameter,  $\gamma_{PA}$ . Initially set to zero,  $\gamma_{PA}$  is updated during training through backpropagation, similar to the Channel Attention Module, but optimized independently for the Pyramid Attention Module.

### 3.3. Feature Fusion and Reconstruction

Within the J-CaPA module, the Pyramid Attention (PA) and Channel Attention (CA) process the input feature map inde-

pendently. The output of PA,  $F_{PA} \in \mathbb{R}^{B \times C \times H \times W}$ , and output of CA,  $F_{CA} \in \mathbb{R}^{B \times C \times H \times W}$ , are fused via element-wise summation:

$$F_{\text{fused}} = F_{PA} + F_{CA}$$

The fused map is then passed through 3x3 convolutional layers to refine the features and capture more details. After the convolutional layers, upsampling layers using bilinear interpolation are applied to restore the feature map to the original input resolution. Finally, a ReLU-activated convolutional layer generates the segmentation mask.

### 3.4. Extended Data Augmentation

Using two attention mechanisms in our model increases the size of the model, requiring an increased amount of training data to support generalization and avoid over-fitting. Thus we extend data augmentation to include CutMix augmentation which combines patches from different images [32]. Segments from one image are randomly cut and pasted onto another, with their respective labels. The size of the segments is varied randomly, covering between 20% to 60% of the image area, ensuring diverse learning scenarios. CutMix was applied to 33% of the images in each training batch to maintain a balance between original and augmented data. For the remaining images in each batch, we applied standard augmentation techniques, such as flipping and rotating.

### 3.5. Data

Experiments in our study use the Synapse multi-organ segmentation dataset, which contains 30 abdominal CT scans. These scans consist of a total of 3,779 axial contrast-enhanced clinical CT images, where each CT scan is composed of multiple slices. The dataset provides annotations for several organs across these scans, including the aorta, gallbladder, left kidney, right kidney, liver, pancreas, spleen, and stomach, along with a ‘none’ label, resulting in a total of nine target classes. We used a preprocessed version of this dataset [14]. We follow prior work to split the 30 scans, with 18 used for training, and the remaining 12 reserved for testing.

### 3.6. Experimental Details

We use a baseline transformer which prior work indicated was the most effective among configurations tested [14]. The specific configuration is called R50-ViT-B\_16. In order to allow a fair comparison across methods, all parameters, including model architecture and training settings, were kept consistent with original specifications. The model was trained for 150 epochs with a batch size of 8 on a single RTX 3080 GPU, taking approximately 2 hours to complete the training.

## 4. RESULTS

We conducted an evaluation to compare the performance of our model to multiple state-of-the-art methods when segmenting organs in abdominal CT scans. Results are provided in Table 1. We follow prior work and report results using the metrics Mean Dice score and Hausdorff Distance (HD95), facilitating a direct comparison with baseline models. Our method outperforms all comparison models on these metrics.

The integration of Joint Channel and Pyramid Attention mechanisms into our architecture significantly enhanced our model’s segmentation capabilities. A higher Mean Dice score reflects better overlap between predicted and ground truth segmentations, while a lower Hausdorff Distance (HD95) indicates more precise organ boundary delineation. Our method achieved a 6.9% improvement in Mean Dice, increasing it to 82.29% and a 39.9% reduction in HD95, lowering it to 19.743 mm, compared to an implementation without the channel and pyramid enhancements, identical to TransUNet in this table.

Figure 2 presents a visual comparison of segmentation performance across cases from the Synapse dataset. The

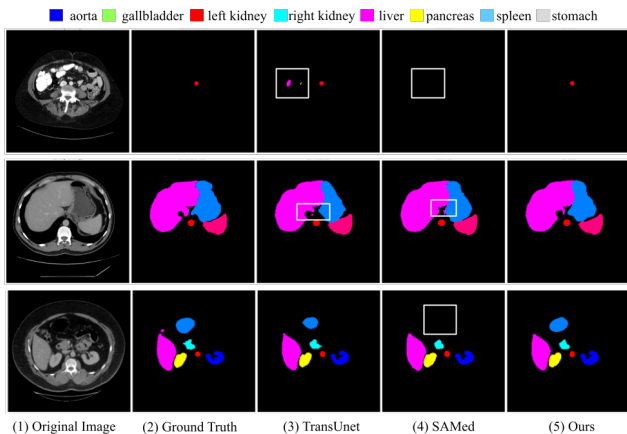


**Fig. 2:** Visual comparison of segmentation results on the Synapse dataset. Each row represents a different case, with the columns showing: (1) the original CT image, (2) ground truth segmentation labels, (3) predictions from TransUNet, and (4) predictions from SAMed (5) predictions from our proposed model.

white boxes highlight areas where TransUNet and SAMed results contain false positives or false negatives, failing to capture certain structures accurately. In contrast, our model demonstrates improved precision by successfully identifying these challenging regions. For instance, in the first row, TransUNet produced a false positive in the liver, while SAMed failed to predict the left kidney. In the last image, SAMed missed the spleen entirely, underscoring our model’s ability to correct these misclassifications.

## 5. ABLATION STUDY

We conducted an ablation study to assess the impact of Channel Attention, Pyramid Attention, and CutMix data augmentation on our model’s performance. The results, shown in Table 2, compare a baseline implementation without our enhancements to the model with each enhancement added. We find that while each of Channel Attention and Pyramid Attention improve on the baseline, neither acting alone performs as well as the Joint Attention model.

Our full model, combining Joint Channel and Pyramid Attention and enhanced data augmentation using CutMix, achieves the best overall performance with a Mean Dice of 82.2% and HD95 of 19.74 mm.

**Table 2:** Ablation study results for Mean Dice score and Hausdorff Distance (HD95).

Model	Mean Dice	Mean HD95
Baseline (without enhancements)	76.90	32.87
Baseline +Channel Attention	79.70	23.56
Baseline +Pyramid Attention	78.14	31.38
Baseline +Joint Attention	80.30	23.73
Baseline +CutMix	79.80	22.69
<b>Ours (Full Model)</b>	<b>82.29</b>	<b>19.74</b>

## 6. CONCLUSION

In this paper, we propose a Transformer-based U-Net model for medical image segmentation, integrating Joint Channel and Pyramid Attention mechanisms (J-CaPA) to improve feature representation. Our approach demonstrates notable improvements in segmentation accuracy and generalization, particularly for challenging organs in abdominal CT scans.

## 7. COMPLIANCE WITH ETHICAL STANDARDS

The Synapse multi-organ segmentation dataset used in this study is publicly available and contains de-identified, anonymized data. No further ethical approval was required.

## 8. ACKNOWLEDGEMENT

We are grateful to Prof. Yuyin Zhou for her guidance and suggestions throughout the duration of this project, and Vanshika Vats for her valuable feedback. No financial conflicts exist.

## 9. REFERENCES

- [1] O. Ronneberger, P. Fischer, and T. Brox, "U-Net: Convolutional Networks for Biomedical Image Segmentation," in *Medical image computing and computer-assisted intervention—MICCAI 2015*, 2015, pp. 234–241.
- [2] J. M. J. Valanarasu, V. A. Sindagi, I. Hacihaliloglu, and V. M. Patel, "KiU-Net: Accurate Segmentation of Biomedical Images using Over-complete Representations," in *Med. Image Comput. Comput.-Assist. Intervent.*, 2020, pp. 363–373.
- [3] Xiao Xiao, Shen Lian, Zhiming Luo, and Shaozi Li, "Weighted Res-UNet for High-Quality Retina Vessel Segmentation," in *2018 9th international conference on information technology in medicine and education (ITME)*. IEEE, 2018, pp. 327–331.
- [4] M. Z. Alom, M. Hasan, C. Yakopcic, T. M. Taha, and V. K. Asari, "Recurrent Residual Convolutional Neural Network based on U-Net (R2U-Net) for Medical Image Segmentation," *arXiv preprint arXiv:1802.06955*, 2018.
- [5] J. Long, E. Shelhamer, and T. Darrell, "Fully Convolutional Networks for Semantic Segmentation," in *Proc. IEEE Conf. Comput. Vis. Pattern Recognit.*, 2015, pp. 3431–3440.
- [6] Z. Zhou, M. M. Siddiquee, N. Tajbakhsh, and J. Liang, "UNet++: A Nested U-Net Architecture for Medical Image Segmentation," in *Deep Learning Med. Image Anal. Multimodal Clin. Decision Support*, 2018, pp. 3–11.
- [7] O. Oktay, J. Schlemper, L. Le Folgoc, M. Lee, M. Heinrich, K. Misawa, K. Mori, S. McDonagh, N. Y. Hammerla, B. Kainz, et al., "Attention U-Net: Learning Where to Look for the Pancreas," *arXiv preprint arXiv:1804.03999*, 2018.
- [8] D. Jha, M. A. Riegler, D. Johansen, P. Halvorsen, and H. D. Johansen, "DoubleU-Net: A Deep Convolutional Neural Network for Medical Image Segmentation," in *Proc. IEEE Int. Symp. Comput.-Based Med. Syst. (CBMS)*, 2020, pp. 558–564.
- [9] D.-P. Fan, G.-P. Ji, T. Zhou, G. Chen, H. Fu, J. Shen, and L. Shao, "PraNet: Parallel Reverse Attention Network for Polyp Segmentation," in *Med. Image Comput. Comput.-Assist. Intervent.*, 2020, pp. 263–273.
- [10] Xiaolong Wang, Ross Girshick, Abhinav Gupta, and Kaiming He, "Non-local Neural Networks," in *Proceedings of the IEEE conference on computer vision and pattern recognition*, 2018, pp. 7794–7803.
- [11] J. Schlemper, O. Oktay, M. Schaap, M. Heinrich, B. Kainz, B. Glocker, and D. Rueckert, "Attention Gated Networks: Learning to Leverage Salient Regions in Medical Images," *Med. Image Anal.*, vol. 53, pp. 197–207, 2019.
- [12] A Vaswani, "Attention Is All You Need," *Advances in Neural Information Processing Systems*, 2017.
- [13] Alexey Dosovitskiy, "An Image is Worth 16x16 Words: Transformers for Image Recognition at Scale," *arXiv preprint arXiv:2010.11929*, 2020.
- [14] J. Chen, Y. Lu, Q. Yu, X. Luo, E. Adeli, Y. Wang, L. Lu, A. L. Yuille, and Y. Zhou, "TransUNet: Transformers Make Strong Encoders for Medical Image Segmentation," *arXiv preprint arXiv:2102.04306*, 2021.
- [15] H. Cao, Y. Wang, J. Chen, D. Jiang, X. Zhang, Q. Tian, and M. Wang, "Swin-Unet: Unet-like Pure Transformer for Medical Image Segmentation," in *Eur. Conf. Comput. Vis.*, 2022, pp. 205–218.
- [16] A. Lin, B. Chen, J. Xu, Z. Zhang, G. Lu, and D. Zhang, "DS-TransUNet: Dual Swin Transformer U-Net for Medical Image Segmentation," *IEEE Trans. Instrum. Meas.*, vol. 71, pp. 1–15, 2022.
- [17] Y. Yang and S. Mehrkanoon, "AA-TransUNet: Attention Augmented TransUNet For Nowcasting Tasks," in *Int. Joint Conf. Neural Netw. (IJCNN)*, 2022, pp. 01–08.
- [18] G. Sun, Y. Pan, W. Kong, Z. Xu, J. Ma, T. Racharak, L.-M. Nguyen, and J. Xin, "DA-TransUNet: Integrating Spatial and Channel Dual Attention with Transformer U-Net for Medical Image Segmentation," *Front. Bioeng. Biotechnol.*, vol. 12, pp. 1398237, 2024.
- [19] A. Kirillov, E. Mintun, N. Ravi, H. Mao, C. Rolland, L. Gustafson, T. Xiao, S. Whitehead, A. C. Berg, W.-Y. Lo, et al., "Segment Anything," in *Proceedings of the IEEE/CVF International Conference on Computer Vision*, 2023, pp. 4015–4026.
- [20] X. Wang, X. Zhang, Y. Cao, W. Wang, C. Shen, and T. Huang, "SegGPT: Towards Segmenting Everything in Context," in *Proc. IEEE/CVF Int. Conf. Comput. Vis.*, 2023, pp. 1130–1140.
- [21] Z. Huang, H. Wang, Z. Deng, J. Ye, Y. Su, H. Sun, J. He, Y. Gu, L. Gu, S. Zhang, et al., "STU-Net: Scalable and Transferable Medical Image Segmentation Models Empowered by Large-Scale Supervised Pre-training," *arXiv preprint arXiv:2304.06716*, 2023.
- [22] Jun Ma, Yuting He, Feifei Li, Lin Han, Chenyu You, and Bo Wang, "Segment Anything in Medical Images," *Nature Communications*, vol. 15, no. 1, pp. 654, 2024.
- [23] Yichi Zhang, Zhenrong Shen, and Rushi Jiao, "Segment Anything Model for Medical Image Segmentation: Current applications and future directions," *Computers in Biology and Medicine*, p. 108238, 2024.
- [24] Xinrong Hu, Xiaowei Xu, and Yiyu Shi, "How to efficiently adapt large segmentation model (SAM) to medical images," *arXiv preprint arXiv:2306.13731*, 2023.
- [25] Kaidong Zhang and Dong Liu, "Customized Segment Anything Model for Medical Image Segmentation," *arXiv preprint arXiv:2304.13785*, 2023.
- [26] E. J. Hu, Y. Shen, P. Wallis, Z. Allen-Zhu, Y. Li, S. Wang, L. Wang, and W. Chen, "LoRA: Low-Rank Adaptation of Large Language Models," *arXiv preprint arXiv:2106.09685*, 2021.
- [27] R. Azad, M. T. Al-Antary, M. Heidari, and D. Merhof, "TransNorm: Transformer Provides a Strong Spatial Normalization Mechanism for a Deep Segmentation Model," *IEEE Access*, vol. 10, pp. 108205–108215, 2022.
- [28] G. Li, D. Jin, Q. Yu, and M. Qi, "IB-TransUNet: Combining Information Bottleneck and Transformer for Medical Image Segmentation," *J. King Saud Univ. Comput. Inf. Sci.*, vol. 35, no. 3, pp. 249–258, 2023.

- [29] J. Fu, J. Liu, H. Tian, Y. Li, Y. Bao, Z. Fang, and H. Lu, "Dual Attention Network for Scene Segmentation," in *Proc. IEEE/CVF Conf. Comput. Vis. Pattern Recognit.*, 2019, pp. 3146–3154.
- [30] Yang Li, Jun Yang, Jiajia Ni, Ahmed Elazab, and Jianhuang Wu, "TA-Net: Triple Attention Network for Medical Image Segmentation," *Computers in Biology and Medicine*, vol. 137, pp. 104836, 2021.
- [31] F. Yu, Y. Zhu, X. Qin, Y. Xin, D. Yang, and T. Xu, "A Multi-Class COVID-19 Segmentation Network with Pyramid Attention and Edge Loss in CT Images," *IET Image Process.*, vol. 15, no. 11, pp. 2604–2613, 2021.
- [32] S. Yun, D. Han, S. J. Oh, S. Chun, J. Choe, and Y. Yoo, "Cut-Mix: Regularization Strategy to Train Strong Classifiers With Localizable Features," in *Proc. IEEE/CVF Int. Conf. Comput. Vis.*, 2019, pp. 6023–6032.